Tribology Letters (2018) 66:17
https://doi.org/10.1007/s11249-017-0970-1

ORIGINAL PAPER

Investigation of Lubricant Transfer and Lubricant Fragmentation in a Hard Disk Drive

Young Woo Seo[1] · **Andreas Rosenkranz**[1] · **Frank E. Talke**[1]

Received: 3 October 2017 / Accepted: 29 November 2017 / Published online: 6 December 2017

Abstract

Lubricant transfer is investigated versus temperature, local pressure change and disk velocity considering lubricant fragmentation for four different types of perfluoropolyether. Lubricant transfer and lubricant fragmentation are found to increase with temperature, local pressure change and velocity of the moving disk. The local pressure change is observed to be the most important parameter accelerating lubricant fragmentation.

Keywords Head–disk interface · PFPE · Lubricant fragmentation · Lubricant transfer · Molecular dynamics

1 Introduction

The reduction in flying height between head and disk has increased the likelihood of intermittent head–disk contacts and lubricant transfer from the disk to the head. Lubricant transfer can occur even in the absence of head–disk contacts, affecting the flying characteristics of the heads and the possibility of catastrophic failure [1].

Lubricant transfer has been addressed in various publications. Deoras and Talke [2] experimentally investigated lubricant transfer and concluded that lubricant thickness and slider skew angle are important parameters for lubricant depletion on the disk surface. Canchi and Bogy [3] observed lubricant transfer in the absence of actual head–disk contact. Ma and Liu [4] suggested that lubricant transfer depends on molecular weight, lubricant thickness and bonding ratio. Pan et al. [5] developed a molecular dynamics model for lubricant transfer and concluded that lubricant transfer increases with local pressure change and lubricant bonding ratio. Seo et al. [6] applied Pan's model [5] to finite width air bearings and observed that lubricant transfer is a function of local pressure change and disk velocity. They also observed that lubricant transfer depends on air bearing convergence angle, functional beads on the disk surface, minimum head–disk spacing and mass of backbone beads.

Chen et al. [7] performed drag tests and observed that high mechanical stress can lead to lubricant fragmentation. Bogy and Bhatia [8] also observed fragmentation of perfluoropolyether lubricant in a tribochamber during drag testing of a head against a disk coated with Zdol. Zhao et al. [9] concluded that the mechanism of lubricant fragmentation is related to low-energy electron emission from rubbing surfaces and mechanical shear stress. Similarly, Tao and Bhushan [10] observed lubricant fragmentation as a consequence of mechanical chain scission and triboelectrical effects. They also noted that relative humidity can affect lubricant fragmentation. Deb Nath and Wong [11] used molecular dynamics to study the effect of temperature on lubricant fragmentation and observed that lubricant fragmentation increases with temperature. Pan et al. [12] used molecular dynamics to study the effect of lubricant fragments on lubricant transfer by assuming a fixed number of lubricant fragments at the start of the simulation. This assumption is equivalent to assuming that dynamic effects are negligible.

In this study, we simulate lubricant transfer and lubricant fragmentation using molecular dynamics, assuming that the number of lubricant fragments is variable. This assumption is equivalent to postulating that dynamic effects are important. Throughout the simulation, we investigate lubricant transfer and lubricant fragmentation as a function of temperature T, local pressure change ΔP and disk velocity V_{disk}.

✉ Frank E. Talke
ftalke@ucsd.edu

[1] Center for Memory and Recording Research, UC San Diego, La Jolla, CA 92093, USA

2 Molecular Dynamics Model

To speed up the numerical calculations, we use the so-called coarse-grained bead spring approach [5, 6]. This approach groups a number of atoms into a "bead," rather than treating each atom at an atomistic level [13]. For instance, a perfluoropolyether chain of Zdol 2000 is modeled as a molecule of ten beads: two functional end beads and eight backbone beads [6].

Figure 1 shows four different types of lubricant molecules used in this study. Type I (Fig. 1a) consists of two functional end beads and eight backbone beads [5, 6], representing a structure similar to Zdol 2000. Type II (Fig. 1b) is a molecule that is twice as long as Type I and has two functional end beads and eighteen backbone beads, representing a structure similar to Zdol 4000. Type III lubricant (Fig. 1c) has two functional end beads, two functional center beads and six non-functional backbone beads [13], representing a structure similar to ZTMD. Lastly, Type IV lubricants (Fig. 1d) consist of four functional end beads and six backbone beads, representing a structure similar to Z-tetraol. Comparing lubricant Types I, III and IV, we observe that each molecule has the same number of beads and molecular weight of 2000 g/mol. However, Type III and IV lubricants have twice the number of functional beads than Type I lubricant. Due to the increased number of functional groups for Type III and IV lubricants, polar interactions between the individual chains are more likely to occur. The Type II lubricant molecule has a molecular weight of 4000 g/mol. In our simulation, a total of 23,000 lubricant beads are modeled, regardless of the type of lubricant used.

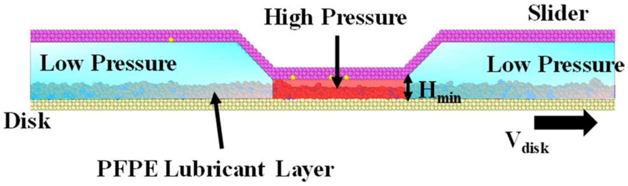

Fig. 2 Schematic of simplified head–disk interface

Figure 2 shows a simplified model of the head–disk interface [6], consisting of low pressure regions at the inlet and outlet of the bearing, and one high pressure region in the center of the bearing to represent the typical pressure distribution under an air bearing surface. The disk velocity V_{disk} and the minimum spacing H_{min} between the head and the disk were chosen to correspond to the actual disk velocity and the minimum flying height found in typical present-day hard disk drives. The disk surface was modeled with functional sites to simulate bonding between lubricant molecules and the disk surface.

Similar to Ref. [6], bead interactions were described using the following potential functions. The 12-6 LJ potential function was used to describe van der Waals forces among the beads [5]. Polar attractions between functional beads were described using the EXP potential function [14]. Bonds among PFPE lubricant beads were modeled using the FENE potential function [15]. In addition, the quartic potential function was used to describe bond breaking [11, 16]. In this study, the molecular dynamics simulations were performed using LAMMPS [17].

Similar to Ref. [6], the simulation was divided into two steps. First, a canonical ensemble (NVT) was assumed. For this system, 140,000 time steps with a step size of 0.005τ were performed. In the second step of the simulation, we

Fig. 1 Four different types of lubricant molecules used in the present molecular dynamics simulation

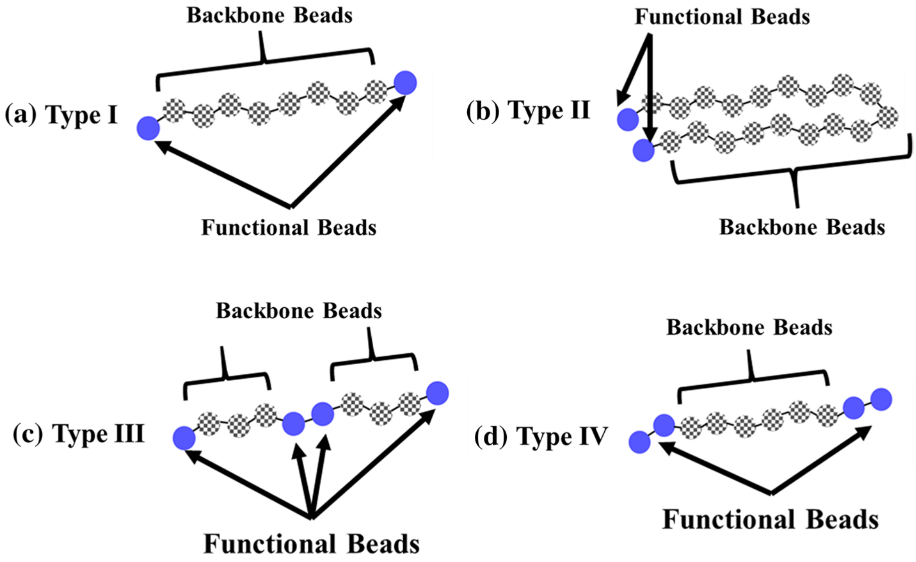

assumed a micro-canonical ensemble (NVE). The Langevin dynamics was used to control the temperature during the simulation [17]. A total of 1,640,000 time steps with a step size of 0.0005τ were performed to simulate lubricant transfer and lubricant fragmentation at the head–disk interface. After this, the head and the disk were separated from each other to a distance of 40σ for post-processing to count the number of transferred lubricant beads and the number of fragmented lubricant chains. Throughout the calculations, we used the LJ units ($\sigma = 0.7$ nm, $\tau \sim 100$ ps and $\varepsilon \sim 10^{-21}$ J) [17].

3 Results and Discussion

Figure 3 gives simulation results for lubricant transfer and lubricant fragmentation versus time for a local pressure change of $\Delta P = 5\varepsilon/\sigma^3$ between the inlet and the center of the bearing, a disk velocity $V_{\text{disk}} = 2.5\sigma/\tau$ (~ 20 m/s), a minimum spacing between the head and the disk of $H_{\min} = 5\sigma$, and a temperature $T = 1.2\varepsilon/\text{k}_\text{B}$, where k_B is the Boltzmann constant. Figure 3a shows the initial state with a thin layer of Type I lubricants on the bottom surface. At $t = 100\tau$ (Fig. 3b), we observe that lubricant molecules accumulate at the converging side of the interface where the pressure changes from low pressure to high pressure (*left* interface of low-to-high pressure region). A lubricant bridge is formed between the head and disk surfaces, similar to the lubricant bridge found by Pan et al. [5] and Seo et al. [6]. The accumulation of lubricant at the converging step increases with time (Fig. 3b–d) and covers the entire converging region after 1,000,000 steps ($t = 500\tau$). In addition to lubricant accumulation, lubricant fragments are formed, as shown by the dots in the highlighted circles on the right-hand side of Fig. 3 (see Fig. 3c, e, f). The number of lubricant fragments in the diverging section of the head is much smaller than the number of adhering lubricant molecules in the converging section.

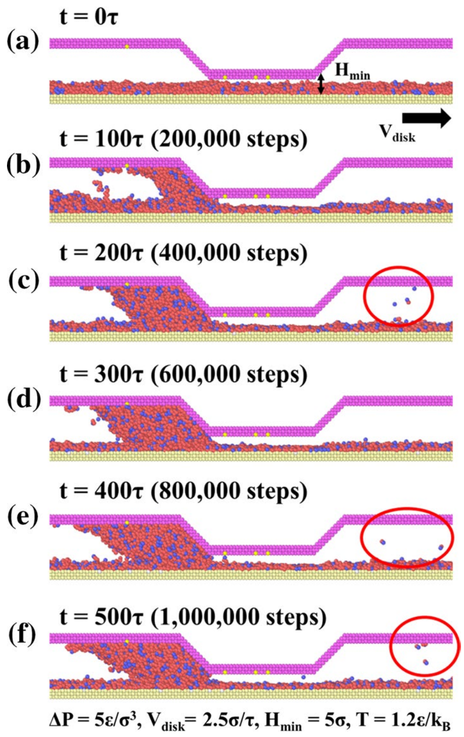

Fig. 3 Molecular dynamics simulation results at different times: **a** $t = 0\tau$, **b** $t = 100\tau$, **c** $t = 200\tau$, **d** $t = 300\tau$, **e** $t = 400\tau$ and **f** $t = 500\tau$ (50 ns)

3.1 Lubricant Transfer

Figure 4 shows molecular dynamics results of lubricant transfer for all four types of lubricants versus temperature (Fig. 4a), local pressure change (Fig. 4b) and disk velocity (Fig. 4c). We observe that lubricant transfer increases for all four types with an increase in temperature (Fig. 4a), local pressure change (Fig. 4b) and disk velocity (Fig. 4c). For Type I lubricants, we observe a slight reduction in lubricant transfer at a temperature of $1.8\varepsilon/\text{k}_\text{B}$, which we believe is due to numerical errors in the simulation. At low temperature, only a few lubricant molecules are seen to transfer to the head for Type I, Type III and Type IV lubricants, while at high temperature lubricant transfer increases sharply before leveling off at values of T exceeding $1.4\varepsilon/\text{k}_\text{B}$ (~ 70 °C). Further investigation is needed in order to fully understand the "leveling off" phenomenon.

Also, at low temperature and low disk velocity, the amount of Type III and IV transferred lubricant molecules is much smaller than that of Types I and II (Fig. 4a, c). This result is related to the fact that Type I and II lubricants have two functional beads, while Type III and IV lubricants have four functional beads (see Fig. 1 for details), i.e., Type III and IV lubricants have stronger bonds with the disk surface than Type I and Type II. Comparing our numerical study with those of others [5, 6, 18, 19], we conclude that our simulations show similar results, i.e., lubricant transfer is reduced with an increase in bond strength of PFPE lubricants on the disk surface. Guo et al. [20], Sonoda et al. [21] and Shirakawa et al. [22] stated that multidentate lubricants with multiple functional beads throughout the lubricant chain and multifunctional lubricants with multiple functional end groups have strong bonding to the disk surface. Similarly, we observe that Type III (multidentate) lubricants and Type IV (multifunctional) lubricants show stronger bonding to the disk surface than Type I and II lubricants.

Type III lubricants have two functional end beads and two functional center beads, while Type IV lubricants have four functional end beads (Fig. 1). Despite these differences, the simulation results were similar for Type III and IV

Fig. 4 Lubricant transfer versus **a** temperature, **b** local pressure change and **c** disk velocity

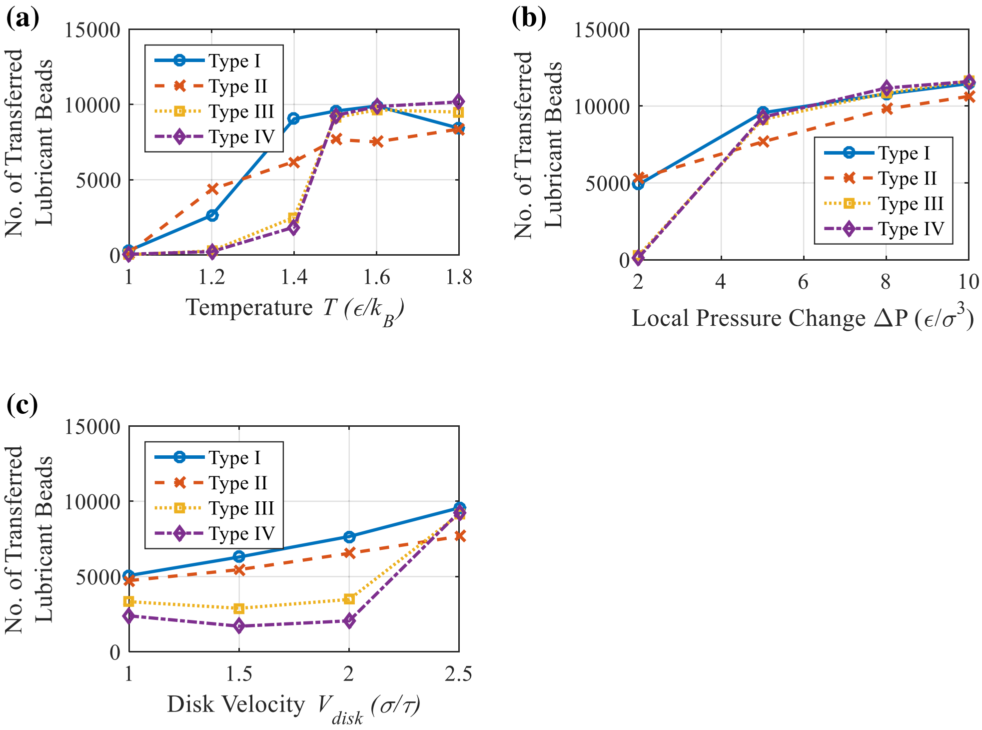

Fig. 5 Lubricant fragmentation versus **a** temperature, **b** local pressure change and **c** disk velocity

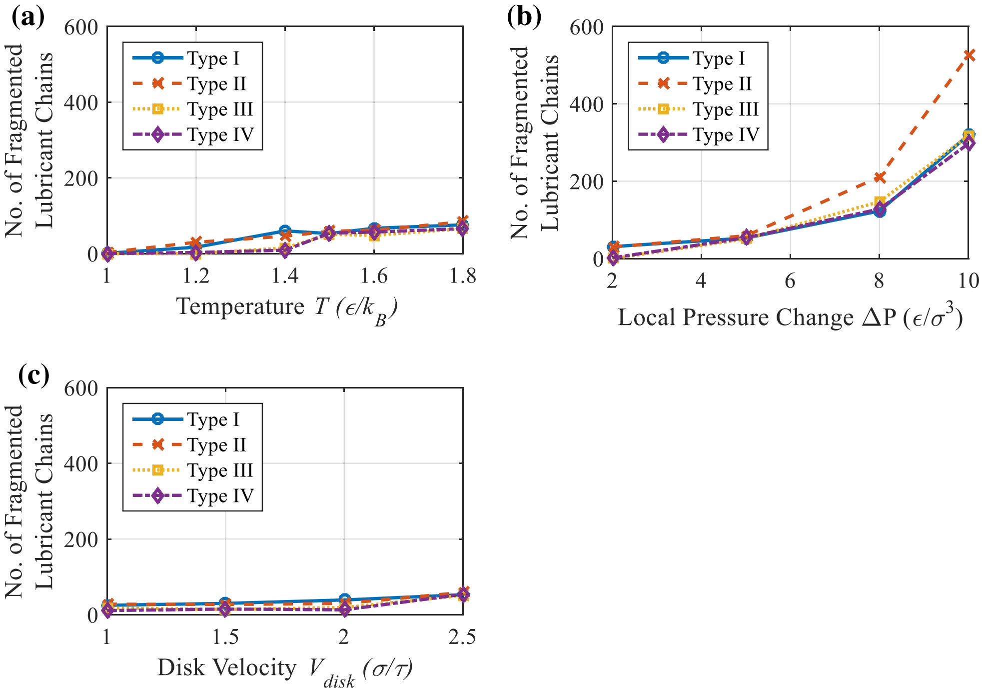

lubricants, suggesting that the location of functional beads (center or end) is of minor importance.

3.2 Lubricant Fragmentation

Figure 5 shows lubricant fragmentation results for all four types of lubricant molecules investigated versus temperature, local pressure change and disk velocity. We note that for all four types, lubricant fragmentation increases with an increase in temperature (Fig. 5a), local pressure change (Fig. 5b) and disk velocity (Fig. 5c). Clearly, lubricant fragmentation is most affected by local pressure change. We also observe that the number of fragmented lubricant chains is largest for Type II (Fig. 5b). This is a consequence of the fact that lubricant chains of Type II are twice as long as Type I with only two functional end beads, i.e., this type of lubricant is prone to fragmentation because of its large chain length. However, this does not imply that the amount of transferred Type II lubricants is larger than that of other lubricant types. In fact, as shown in Fig. 4b, the number of transferred Type II lubricant beads is smaller than that of other lubricant types at a local pressure change of $\Delta P = 5\varepsilon/\sigma^3$, $8\varepsilon/\sigma^3$ and $10\varepsilon/\sigma^3$, respectively. Pan et al. [12] concluded that lubricant fragmentation is one of the reasons for lubricant transfer. In our study, we observe that lubricant transfer from the disk to the head appears to be caused mainly by the formation of a lubricant bridge as shown in Fig. 3.

Lubricant fragmentation is most significantly affected by local pressure change as shown in Fig. 5b. Since shear stress at the wall is related to local pressure change ΔP, it is apparent that lubricant fragmentation is a function of the shear stress. The pressure gradient and the shear stress in an air bearing at high Knudsen numbers are related by [23–25]:

$$\tau_{\mathrm{w}}\big|_{\mathrm{disk}} = -\rho\lambda\sqrt{\frac{\mathrm{R}T_0}{2\pi}}\frac{U}{2\lambda + h} - \frac{h}{2}\frac{\mathrm{d}p}{\mathrm{d}x} \tag{1}$$

where $\mathrm{d}p/\mathrm{d}x$ is the air bearing pressure gradient, ρ is the density of air, λ is the mean free path of air molecules, R is the specific gas constant, T_0 is the ambient temperature, U is the disk velocity and h is the spacing between the head and the disk. Equation (1) shows that the shear stress depends both on the disk velocity U and on the pressure gradient $\mathrm{d}p/\mathrm{d}x$.

Wei et al. [26] reported that shear stress can cause lubricant fragmentation by stretching the intramolecular bond until it breaks. In our molecular dynamics simulation, the mechanism for bond breakage is simulated in which the intramolecular bond breaks when the bond length is extended beyond the cutoff distance. Assuming that the local pressure change ΔP in our molecular dynamics simulation corresponds to the pressure gradient $\mathrm{d}p/\mathrm{d}x$ of the air bearing surface, it follows that the shear stress on the disk surface is related to the local pressure change ΔP. With an increase in local pressure change, the shear stress increases, and an increase in shear stress leads to an increase in lubricant fragmentation.

Equation (1) shows that shear stress in an air bearing depends on the pressure gradient and the disk velocity. Our simulation results, on the other hand, showed that disk velocity V_{d} has a smaller effect on lubricant fragmentation (Fig. 5c) than the local pressure change ΔP. We believe that this can be explained by the fact that the range of disk velocities investigated was smaller in comparison with the range of local pressure change, i.e., velocity V_{d} was investigated from $1.0\sigma/\tau$ to $2.5\sigma/\tau$ ($\frac{\max}{\min} = 2.5$), while ΔP was investigated from $2\varepsilon/\sigma^3$ to $10\varepsilon/\sigma^3$ ($\frac{\max}{\min} = 5.0$). Further investigations beyond the scope of this paper would be needed to explore this effect in more detail.

4 Summary

Molecular dynamics simulation was carried out to study lubricant transfer and lubricant fragmentation for four different lubricant types. We conclude that

1. Lubricant transfer is a function of temperature, local pressure change and disk velocity.
2. Fewer lubricant beads are transferred at low temperature for Type III (two functional end beads and two functional center beads) and Type IV (four functional end beads) lubricants compared to Type I or Type II lubricants.
3. Type II lubricant chains fragment more easily with high local pressure change than other lubricant types.
4. Lubricant fragmentation is most significantly affected by local pressure change. A further investigation is needed in order to fully understand the effect of disk velocity on lubricant fragmentation.

Our coarse-grained bead spring model addresses only a limited number of parameters affecting lubricant transfer, and additional parameters such as humidity or lubricant chemistry can play a role in lubricant transfer. A full atomistic model would be necessary in order to include those additional parameters on lubricant transfer and fragmentation at the head–disk interface.

Acknowledgements Andreas Rosenkranz acknowledges the Feodor Lynen Fellowship of the Alexander von Humboldt foundation and support from Prof. Talkie's tribology funds. We also would like to express our gratitude to Karcher Morris for helpful discussions.

References

1. Ambekar, R.P., Bogy, D.B., Bhatia, C.S.: Lubricant depletion and disk-to-head lubricant transfer at the head–disk interface in hard disk drives. J. Tribol. **131**(3), 031901 (2009)
2. Deoras, S.K., Talke, F.E.: Slider–lubricant interactions for low flying sliders. IEEE Trans. Magn. **39**(5), 2471–2473 (2003)
3. Canchi, S.V., Bogy, D.B.: Experiments on slider–lubricant interactions and lubricant transfer using TFC sliders. Microsyst. Technol. **18**(9–10), 1517–1523 (2012)
4. Ma, Y., Liu, B.: Lubricant transfer from disk to slider in hard disk drives. Appl. Phys. Lett. **90**(14), 143516 (2007)
5. Pan, D., Ovcharenko, A., Tangaraj, R., Yang, M., Talke, F.E.: Investigation of lubricant transfer between slider and disk using molecular dynamics simulation. Tribol. Lett. **53**(1), 373–381 (2014)
6. Seo, Y.W., Pan, D., Ovcharenko, A., Yang, M., Talke, F.E.: Molecular dynamics simulation of lubricant transfer at the head–disk interface. IEEE Trans. Magn. **50**(11), 1–4 (2014)
7. Chen, C.Y., Fong, W., Bogy, D.B., Bhatia, C.S.: Lubricant thickness effect on tribological performance of ZDOL lubricated disks with hydrogenated overcoats. Tribol. Lett. **7**(1), 1–10 (1999)
8. Bogy, D.B., Bhatia, C.S.: The fragmentation mechanisms and thermal stability of ZDOL lubricant on hydrogenated carbon overcoats. Technical Briefs, p. 458 (2000)
9. Zhao, X., Bhushan, B., Kajdas, C.: Lubrication studies of head–disk interfaces in a controlled environment Part 2: degradation mechanisms of perfluoropolyether lubricants. Proc. Inst. Mech. Eng. Part J J. Eng. Tribol. **214**(6), 547–559 (2000)
10. Tao, Z., Bhushan, B.: Bonding, degradation, and environmental effects on novel perfluoropolyether lubricants. Wear **259**(7), 1352–1361 (2005)
11. Deb Nath, S.K., Wong, C.H.: Study of the thermal decomposition of PFPEs lubricants on a thin DLC film using finitely extensible nonlinear elastic potential based molecular dynamics simulation. J. Nanotechnol. **2014**, 390834 (2014). https://doi.org/10.1155/2014/390834
12. Pan, D., Ovcharenko, A., Peng, J.P., Jiang, H.: Effect of lubricant fragments on lubricant transfer: a molecular dynamics simulation. IEEE Trans. Magn. **50**(9), 1–5 (2014)
13. Jhon, M.S., Chung, P.S., Smith, R.L., Biegler, L.T.: A description of multiscale modeling for the head-disk interface focusing on bottom-level lubricant and carbon overcoat models. Adv. Tribol. **2013**, 794151 (2013). https://doi.org/10.1155/2013/794151
14. Weaver, J.F., Carlsson, A.F., Madix, R.J.: The adsorption and reaction of low molecular weight alkanes on metallic single crystal surfaces. Surf. Sci. Rep. **50**(4), 107–199 (2003)
15. Sexton, B.A., Hughes, A.E., Avery, N.R.: A spectroscopic study of the adsorption and reactions of methanol, formaldehyde and methyl formate on clean and oxygenated Cu (110) surfaces. Surf. Sci. **155**(1), 366–386 (1985)
16. Stevens, M.J.: Interfacial fracture between highly cross-linked polymer networks and a solid surface: effect of interfacial bond density. Macromolecules **34**(8), 2710–2718 (2001)
17. Plimpton, S.: Fast parallel algorithms for short-range molecular dynamics. J. Comput. Phys. **117**(1), 1–19 (1995). http://lammps.sandia.gov/index.html
18. Marchon, B.: Lubricant design attributes for subnanometer head–disk clearance. IEEE Trans. Magn. **45**(2), 872–876 (2009)
19. Li, N., Meng, Y., Bogy, D.B.: Effects of PFPE lubricant properties on the critical clearance and rate of the lubricant transfer from disk surface to slider. Tribol. Lett. **43**(3), 275–286 (2011)
20. Guo, X.C., Knigge, B., Marchon, B., Waltman, R.J., Carter, M., Burns, J.: Multidentate functionalized lubricant for ultralow head/disk spacing in a disk drive. J. Appl. Phys. **100**(4), 044306 (2006)
21. Sonoda, K., Shirakawa, D., Yamamoto, T., Itoh, J.: The tribological properties of the new structure lubricant at the head–disk interface. IEEE Trans. Magn. **43**(6), 2250–2252 (2007)
22. Shirakawa, D., Sonoda, K., Ohnishi, K.: A study on design and synthesis of new lubricant for near contact recording. IEEE Trans. Magn. **43**(6), 2253–2255 (2007)
23. Fukui, S., Kaneko, R.: Analysis of ultra-thin gas film lubrication based on the linearized Boltzmann equation: influence of accommodation coefficient. JSME Int. J. **30**(268), 1660–1666 (1987)
24. Sone, Y.: Molecular Gas Dynamics: Theory, Techniques, and Applications. Springer, Berlin (2007)
25. Liu, N., Bogy, D.B.: Air-bearing shear force in the head–disk interface of hard disk. Tribol. Lett. **35**(2), 121–125 (2009)
26. Wei, J., Fong, W., Bogy, D.B., Bhatia, C.S.: The decomposition mechanisms of a perfluoropolyether at the head/disk interface of hard disk drives. Tribol. Lett. **5**(2), 203–209 (1998)